A SIMPLIFIED MODEL OF DISTRIBUTED PARAMETER SYSTEMS

M. Shirvani

School of Science and Technology
Niigata University
Niigata, Japan

M. Inagaki and T. Shimizu

Department of Materials and Chemical Engineering
Niigata University
Niigata, Japan

Abstract A generalized simplified model for describing the dynamic behavior of distributed parameter systems is proposed. The various specific characteristics of gain and phase angle of distributed parameter systems are investigated from frequency response formulation and complex plane representation of the proposed simplified model. The complex plane investigation renders some important inequality constraints regarding the transcendental characteristics of phase angle. In this way it become possible to classify the various possible phase angle characteristics of these systems. The proposed generalized simplified model is simulated to some actual process systems for further confirmation of the simplification capability of the model and the reuslts of simulation are discussed based on the conclusions of dynamic behavior investigations.

Key Words Distributed Parameter Systems, Frequency Response, Sten Response, Simulation

چکیده یک مدل عمومی ساده برای نمایش رفتار دینامیکی سیستمهای با پارامتر گسترده ارائه شده است. خصوصیات ویژه مربوط به بهره و زاویه فاز سیستمهای با پارامتر گسترده از روی فرمولاسیون پاسخ فرکانسی و نمایش مدل ساده پیشنهاد شده روی محورهای مختلط بررسی شده است. از بررسی مدل در محورهای مختلط بعضی محدودیتهای نامعادله ای مهم برای توجیه رفتارهای پیچیده زاویه فاز بدست آمده است. بدین طریق این امکان حاصل شده است که خصوصیات مختلف زاویه فاز این سیستمها طبقه بندی شود. مدل ساده و عمومی پیشنهاد شده توسط تعدادی از سیستمهای حقیقی شبیه سازی شده اند تا قابلیت ساده سازی مدل مورد بررسی و تأیید قرار گیرد، ودر عین حال نتایج حاصل از شبیه سازی ازروی استنتاجات مربوط به بررسی رفتار دینامیکی مورد بحث و بررسی قرار گرفته است.

INTRODUCTION

Describing the dynamic behavior of systems by simple rational transfer function models is a well-known practice which has been developed and used frequently. Almost a first or second-order rational transfer function or at most a third-order one, which may include a time-delay element, seems to be sufficient for describing the dynamic behavior of many process systems, especially those of lumped parameter behavior.

Although in many cases low-order rational transfer functions are sufficient for this purpose, due to the practical existence of more complex systems, such as boilers, some methods have also been developed for the simplification of such systems by higher-order transfer functions [1,2,3].

The general high-order rational transfer function model for such cases is in the form

$$F(s) = K. \prod_{j=1}^{m} (s-z_j)/\prod_{i=1}^{n} (s-p_i). \qquad (1)$$

In some distributed parameter process systems such as heat exchangers, heat pipes, tubular reactors, packed towers etc., the behavior of the system is so complicated that even the high-order rational transfer functions are not sufficient for use. Still, in distributed parameter systems the problem is more serious than ordinary "time-delay included rational transfer functions" due to the appearance of periodical resonances in their frequency response which may be accompanied by nonminimum phase behavior.

Concerning the step response and frequency response of these systems the following special features may be summarised [4,5,6]:

1) There may appear an abrupt change in the slope of step response in some of these systems. Sometimes the slope can switch signs, while in some cases this abrupt change in slope does not appear.

2) Some of these systems exhibit large phase lags at high frequencies, indicating nonminimum phase behavior. The nonminimum phase behavior may or may not include oscillations.

3) Some distributed parameter systems exhibit limited oscillating phase angle behavior at high frequencies without decreasing continually in a nonminimum phase behavior.

4) Sometimes the minimum or nonminimum phase behavior of the system switches sign at a certain fequency.

5) In the procedure of controller design for these systems, the time-delay element in the model of the system can not be recognized explicity from the model, while in the existing methods for controller design of time-delay included models, the minimum and nonminimum phase parts of the model must be explicitly recognized.

Except for the last item, so far no unique answer or expression to the above problems has been presented in the literature in spite of the great confusion which arises in using the dynamic models of these systems.

Table 1 includes a summation of various models which are used or mentioned in the literature as suitable models for describing dynamic behavior of distributed parameter

TABLE 1.A Summary of Different Models Adopted for Distributed Parameter Systems

	Either proposed or used for simulation or theoretically-derived models: G(s)	$\frac{\text{output}}{\text{input}}$	Number of parameters	Applied for process	Reference number
1.	$\frac{K.e^{-\tau s}}{1+T_1 s}+\frac{1-K}{1+T_2 s}$		4	heat pipe	[7]
2.	$\frac{K_1.e^{-\tau_1 s}}{1+T_1 s}+\frac{K_2.e^{-\tau_2 s}}{1+T_2 s}$	$\frac{\text{temperature}}{\text{velocity}}$	6	heat exchanger	[8]
3.	$\frac{P(s).e^{-\tau s}-1}{Q(s)}$ P(s): Third-order polynomial of "s" Q(s): Fifth-order polynomial of "s"		derived model	fluidized bed calciner	[4,5,6]
4.	$\frac{K(1-a.e^{-\tau s})}{(1+T_1 s)(1+T_2 s)}$, $a<1$		5	—	[9]
5.	$K(s).[1-e^{-\tau s}]$	$\frac{\text{temp.}}{\text{velocity}}$	derived model	steam-liquid heat exchg.	[10]

process systems. In fact much more complicated models also appear in the literature but these are not mentioned in this table.

The unique feature of all of the above models in this table is that they are parallel combinations of two rational transfer functions, one of which includes a time-delay element.

OBJECTIVES

Here as a generalized simplified model for describing the dynamic behavior of distributed parameter systems the transfer function model in Equation 2 is used for investigating the specific characteristics of these systems.

$$G(s) = g_a(s) + g_b(s) \tag{2}$$

where

$$g_a(s) = K_1 . e^{-\tau_1 s} / Q_a(s) \; ; \; g_b(s) = K_2 . e^{-\tau_2 s} / Q_b(s) .$$

This model is an adapted form of all the models in Table 1. Indeed it is a generalized form of model number 2 in the above table which has been used by the authors for simulation to a heat exchanger frequency response data.

If necessary $Q_a(s)$ and $Q_b(s)$ may be some irrational functions of "s", but for the purpose of simplification in process systems they are almost enough to be polynomials, $Q_{am}(s)$ and $Q_{bn}(s)$, with the orders "m" and "n" respectively. In most cases for the purpose of obtaining an applicable simplified model, the polynomials $Q_{am}(s)$ and $Q_{bn}(s)$ are enough to have a maximum degree of 2.

The objective here is to carry out investigations to answer the first four essential questions related to the unknown characteristics of distributed parameter systems. This is done on the simplified model in Equation 2 since the frequency response verification of the model has revealed its good capability to describe the above-mentioned transcendental characteristics of these systems. Also in order to further confirm the ability of the model, some more simulations are carried out here in addition to the existing results in the literature.

FREQUENCY RESPONSE FORMULATION

As a starting point for investigating the dynamic behavior of the model, equations of gain and phase angle are obtained for the general case where $Q_a(s)$ and $Q_b(s)$ are some irrational or rational (polynomial) functions of "s".

$$|G(j\omega)| = \sqrt{(R_a + R_b)^2 + (I_a + I_b)^2} \tag{3}$$

$$\angle G\,(j\omega) = \tan^{-1} \frac{I_a + I_b}{R_a + R_b} \tag{4}$$

R_a, I_a, R_b, and I_b are real and imaginary parts of $\mathbf{g_a}(j\omega)$ and $\mathbf{g_b}(j\omega)$ respectively. This method of analysis may be used for the general case where $Q_a(s)$ and $Q_b(s)$ are irrational functions as well as the simpler cases where they are polynomials of "s".

A simpler yet more straightforward method is based on complex plane representation shown in Figure 1. This is also applicable to irrational $Q_a(s)$ and $Q_b(s)$ as well as rational ones. In Figure 1 vectors **a**, **b** and **c** are representatives of $\mathbf{g_a}(j\omega)$, $\mathbf{g_b}(j\omega)$ and $\mathbf{G}(j\omega)$ respectively. They are used here for simplification in writing the formulas and they have the same subscripts as their respective function. For example $\mathbf{a}_{ir}$ together with α_{ir} shows that $Q_a(s)$ is irrational or $\mathbf{c}_{2,1}$ (numerical subscripts indicate the order of polynomials $Q_a(s)$ and $Q_b(s)$ respectively) is representative of $G_{2,1}(s)$, i.e., $\mathbf{a} = \mathbf{a}_2 = \mathbf{g}_{a2}(j\omega)$, $\alpha = \alpha_2 = \angle \mathbf{g}_{a2}(j\omega)$, $\mathbf{b} = \mathbf{b}_1 = \mathbf{g}_{b1}(j\omega)$, $\beta = \beta_1 = \angle \mathbf{g}_{b1}(j\omega)$, $\mathbf{c} = \mathbf{c}_{2,1} = \mathbf{G}_{2,1}(j\omega)$ and $\gamma = \gamma_{2,1} = \angle \mathbf{G}_{2,1}(j\omega)$.

From the gains of vectors **a** and **b** as well as their angles with real axis the gain and phase angle of **c** can be obtained. $\mathbf{G}(j\omega)$ may be written as:

$$\mathbf{G}(j\omega) = K_1 e^{-\tau_1 j\omega} / (U_a + jV_a) + K_2 e^{-\tau_2 j\omega} / (U_b + jV_b), \tag{5}$$

where U_a, U_b, V_a and V_b are real and imaginary parts of $\mathbf{Q_a}(j\omega)$ and $\mathbf{Q_b}(j\omega)$ respectively. Thus, gain and phase

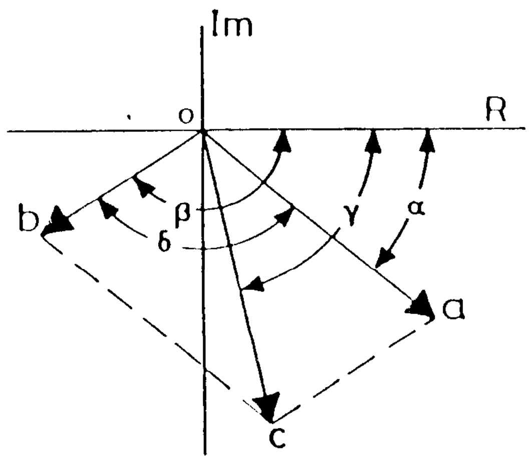

$$|c|^2 = |a|^2 + |b|^2 + 2|a||b|.\cos\delta$$

Figure 1. Complex plane representation of the simplified model in terms of vector summation principle

angle of G(jω) will be obtained straightly from Equation 3 and Figure 1 as:

$$|c| = |G(j\omega)|$$

$$= \sqrt{|a|^2 + |b|^2 + \frac{2K_1K_2}{|K_1||K_2|}|a||b|\cos(\beta-\alpha)} \quad (6)$$

$$\angle c = \angle G(j\omega)$$

$$= \tan^{-1}\frac{(K_1/|K_1|)|a|\sin\alpha + (K_2/|K_2|)|b|\sin\beta}{(K_1/|K_1|)|a|\cos\alpha + (K_2/|K_2|)|b|\cos\beta}, \quad (7)$$

where

$$|a| = |g_a(j\omega)| = \frac{|K_1|}{\sqrt{U_a^2 + V_a^2}}; \ \alpha = -\omega\tau_1 - \tan^{-1}(V_a/U_a);$$

$$|b| = |g_b(j\omega)| = \frac{|K_2|}{\sqrt{U_b^2 + V_b^2}}; \ \beta = -\omega\tau_2 - \tan^{-1}(V_b/U_b);$$

$$\delta = \beta - \alpha = \omega(\tau_1 - \tau_2) + \tan^{-1}(V_a/U_a) - \tan^{-1}(V_b/U_b).$$

In the above expressions the terms $K_1/|K_2|$ and $K_2/|K_2|$ are added for providing a generalization in the equations for the conditions where K_1 and K_2 are negative values. Otherwise one must be careful to insert "$-\pi+\alpha$" instead of "α" when $K_1<0$ and "$-\pi+\beta$" instead of "β" when $K_2<0$ in equations of frequency response. Equations 6 and 7 describe the gain and phase angle of the model in a unified manner for any form of $Q_a(s)$ and $Q_b(s)$.

CHARACTERISTICS OF GAIN

Resonance characteristics of gain are explicitly recognized from Equation 6. At low frequencies (where ω approaches zero) gain approaches

$$|c| = |K_1 + K_2|. \quad (8)$$

By considering the maximum and minimum amount of the cosine term in Equation 6, two upper and lower envelopes of the gain may be expressed as:

$E_u = \max |a| + |b|$	upper envelope	(9 a)
$E_l = \min \| |a| - |b| \|$	lower envelope	(9 b)

At high frequencies, these envelopes of gain will approach two separate straight asymptotes in a log-log scale. Mathematical expression of the asymptotes can be obtained by ignoring the low-value terms of equation of gain at high frequencies. For a $G_{m,n}(s)$ simplified model at high frequencies

$$|c_{m,n}|$$

$$= \sqrt{\frac{K_1^2}{\omega^{2m}T_1^{2m}} + \frac{K_2^2}{\omega^{2n}T_2^{2n}} + \frac{2K_1K_2}{\omega^m T_1^m \omega^n T_2^n}\cos[\omega(\tau_1 - \tau_2)]}\ . \quad (10)$$

Thus

$$N_{m,n} \le |c_{m,n}| \le M_{m,n} \quad (11)$$

where

$$N_{m,n} = \min\left[\left|\frac{K_1}{(T_1\omega)^m} - \frac{K_2}{(T_2\omega)^n}\right|, \left|\frac{K_1}{(T_1\omega)^m} + \frac{K_2}{(T_2\omega)^n}\right|\right]$$

$$M_{m,n} = \max \left[\left| \frac{K_1}{(T_1\omega)^m} - \frac{K_2}{(T_2\omega)^n} \right| , \left| \frac{K_1}{(T_1\omega)^m} + \frac{K_2}{(T_2\omega)^n} \right| \right]$$

In the above equations T_1 and T_2 are the parameters of $g_{am}(s)$ and $g_{bn}(s)$, where the polynomials $Q_{am}(s)$ and $Q_{bn}(s)$ are in the form

$$Q_{am}(s)= (T_1s)^m + c_{a1} (T_1s)^{m-1} + ... + 1 \qquad (12\ a)$$

$$Q_{bn}(s)= (T_2s)^n + c_{b1} (T_2s)^{n-1} + ... + 1, \qquad (12\ b)$$

and $c_{a1}, c_{a2}, ...$ and $c_{b1}, c_{b2}, ...$ are the constants of polynomials. The vertical distance between the two asymptotes is

$$\triangle_{m,n} = M_{m,n} - N_{m,n}. \qquad (13)$$

Figure 2 represents the envelopes of gain for a $G_{1,1}(s)$ model. The gain of model oscillates around the gain of the "higher gain element of the model". This is the straight implicit concept of Equation 11. Another important factor identified from this equation, is that the slope of asymptotes for a $G_{1,1}(s)$ model is -20dB/dec and for a $G_{2,2}(s)$ model it will be -40dB/dec.

CHARACTERISTICS OF PHASE ANGLE

With regard to the phase angle, although its specific characteristics are very important, nothing can be understood explicitly from Equation 7. Actually, this kind of behavior which includes maximum and minimum points has been observed for phase angle by plotting the Bode

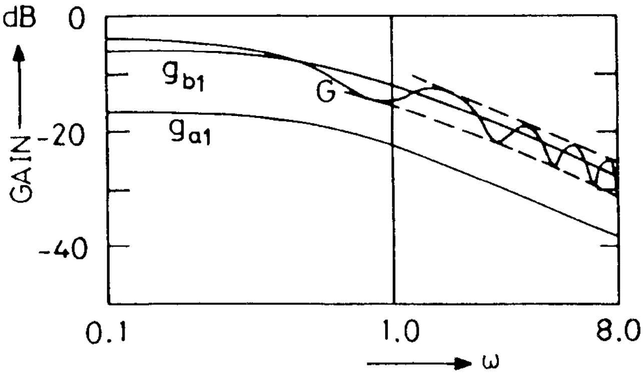

Figure 2. Upper and lower envelopes of gain for a $G_{1,1}(s)$ model

diagram of the model for different amounts of the parameters of models $G_{m,n}(s)$; m= 1,2,3 and n= 1,2,3.

A discussion about this problem is possible by use of complex plane representation of the model.

Complex Plane Investigation of the Characteristics of Phase Angle

Figures 3 and 4 are prepared to show two important cases (or forms), [a] and [b], which can possibly occur or phase angle of **c** due to the rotation of constituent vectors **a** and **b**. These serial figures are drawn at certain arbitrary frequencies such that the position of vectors can show the originality of arising various conditions of phase angle of model during the rotation of vectors. In both figures it is supposed that the vector **a** is in condition of phase lead with respect to **b**; that is vector **a** is slower in rotation than **b**. The difference between the two cases [a] and [b] is only in the lengths (gains) of vectors **a** and **b**.

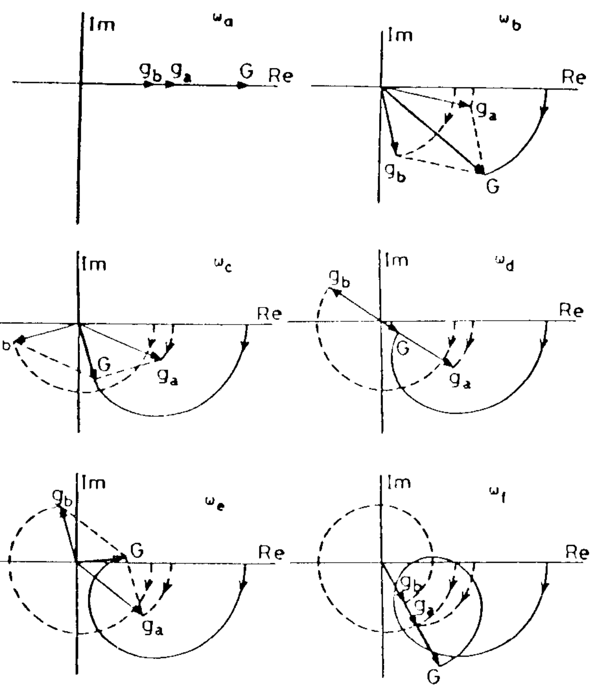

Figure 3. Complex plane representation of vectors at some discrete ω for case [a], $|a| / |b| > 1.0$

$K_1= 0.5$ $T_1= 0.2$ $\tau_1= 0.1$

$K_2= 0.3$ $T_2= 0.3$ $\tau_2= 1.6$

$Q_a(s)= 1 + T_1s$ $Q_b(s)= 1 + T_2s$

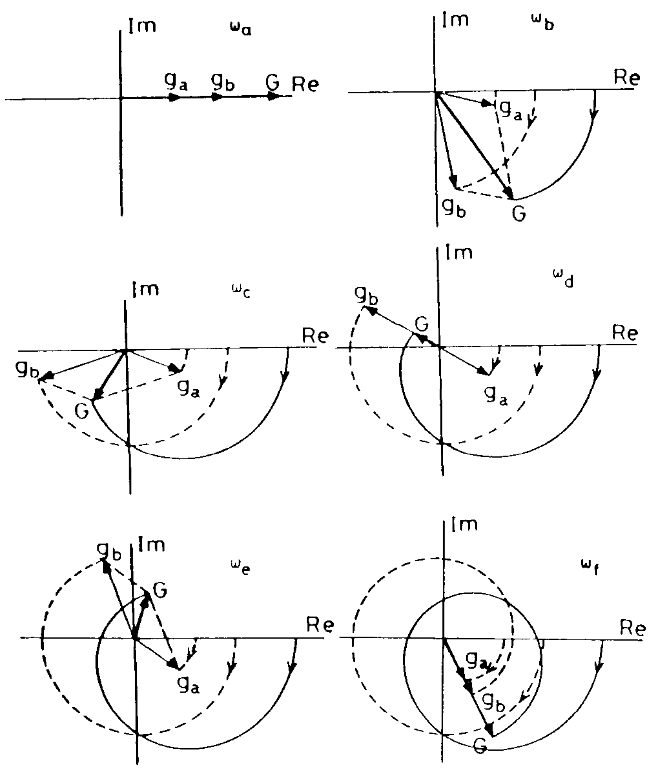

Figure 4. Complex plane representation of vectors at some discrete ω for case [b], $|a| / |b| < 1.0$

$K_1 = 0.3$ $T_1 = 0.2$ $\tau_1 = 0.1$
$K_2 = 0.5$ $T_2 = 0.3$ $\tau_2 = 1.6$
$Q_a(s) = 1 + T_1 s$ $Q_b(s) = 1 + T_2 s$

Close investigation of the above figures reveals that the key point of difference between them is at ω_d where the two vectors **a** and **b** are located in opposite direction with respect to each other and the gain of model "**|c|**" is in its minimum amount. The figures infer that in case [a], Figure 6, with increasing ω, vector **c** oscillates around vector **a** while in case [b], Figure 8, the oscillations are around vector **b**.

In the sense of Bode diagram this means that the maximum and minimum points of the phase angle of model are located around the phase angle of $g_a(s)$ in case [a], and around the phase angle of $g_b(s)$ in case [b]. Therefore, if it is supposed that $g_a(s)$ is a minimum phase transfer function (i.e., $\tau_1 = 0$) and $g_b(s)$ is a nonminimum phase transfer function, then the model G(s) will have a minimum phase characteristic for the condition of case [a], and nonminimum phase characteristic for the condition of case [b]. Regarding the complicated characteristics of distributed parameter systems that are known to be able to show minimum as well as nonminimum phase behavior [4,5,6] the above conclusions are very important.

Some example frequency responses and vector dia-

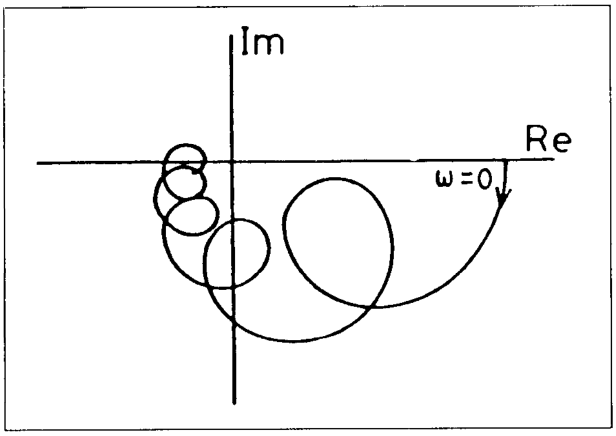

Figure 5. Vector diagram of model for case [a]

$K_1 = 0.5$ $T_1 = 0.2$ $\tau_1 = 0.1$
$K_2 = 0.3$ $T_2 = 0.3$ $\tau_2 = 1.6$
$Q_a(s) = 1 + T_1 s$ $Q_b(s) = 1 + T_2 s$

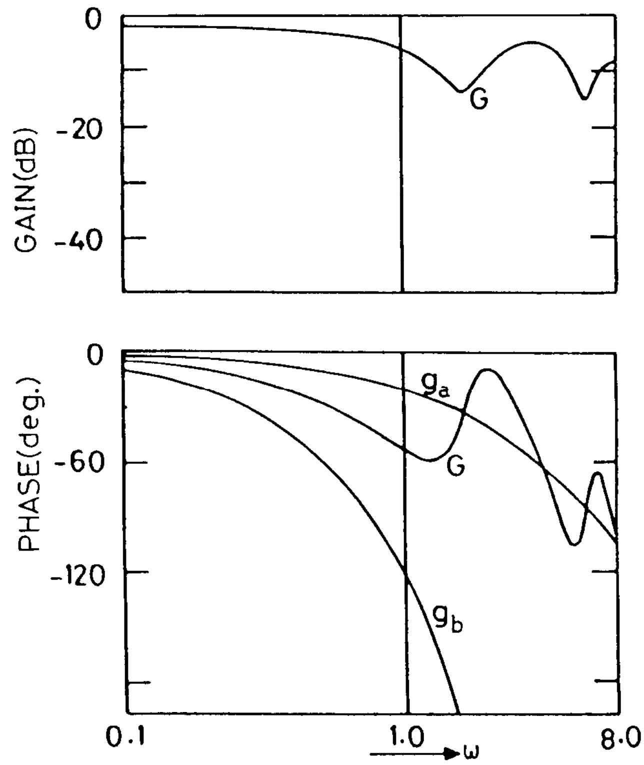

Figure 6. Frequency response of model for case [a]

$K_1 = 0.5$ $T_1 = 0.2$ $\tau_1 = 0.1$
$K_2 = 0.3$ $T_2 = 0.3$ $\tau_2 = 1.6$
$Q_a(s) = 1 + T_1 s$ $Q_b(s) = 1 + T_2 s$

grams are shown in Figures 5-8 for the two cases.

In addition to the above two cases another case, named case [c], is recognizable. This case will be considered for the special condition in which **| a | = | b |**. Frequency response and vector diagrams of this case are shown in Figures 9 and 10. As with case [a], in this case also vector **c** oscillates around **a**, but the length of vector **c** becomes zero at ω_n. As a result, the phase angle becomes indefinite at the point of minimum gain and a jump of +180 deg. appears at this point.

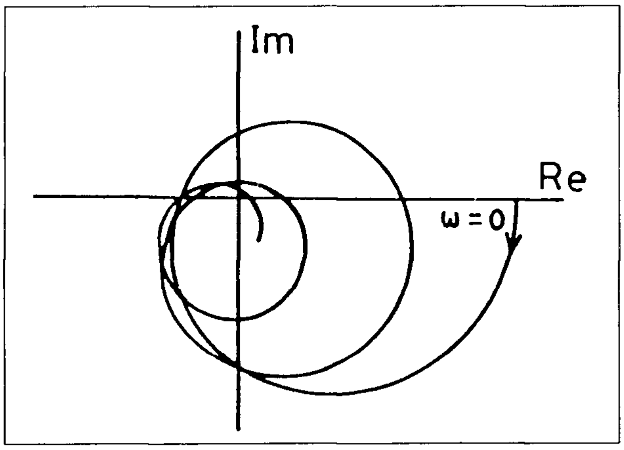

Figure 7. Vector diagram of model for case [b]

$K_1 = 0.3$ $T_1 = 0.2$ $\tau_1 = 0.1$

$K_2 = 0.5$ $T_2 = 0.3$ $\tau_2 = 1.6$

$Q_a(s) = 1 + T_1 s$ $Q_b(s) = 1 + T_2 s$

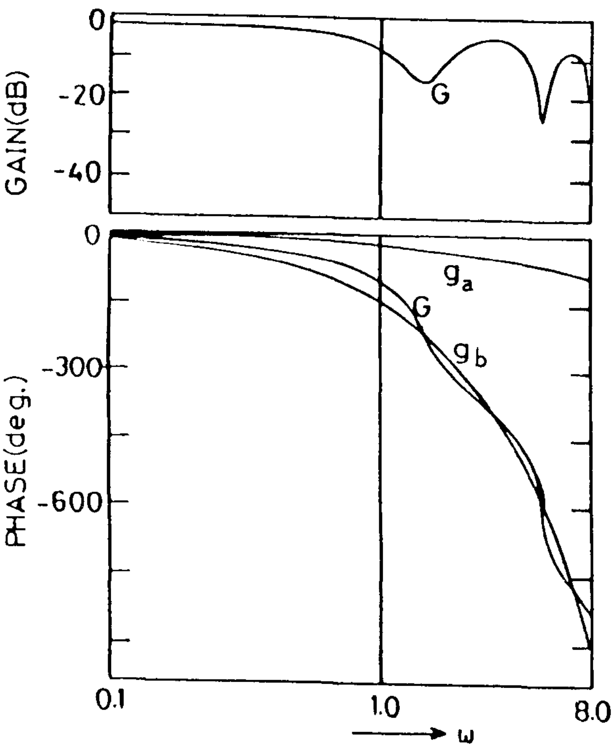

Figure 8. Frequency response of model for case [b]

$K_1 = 0.3$ $T_1 = 0.2$ $\tau_1 = 0.1$

$K_2 = 0.5$ $T_2 = 0.3$ $\tau_2 = 1.6$

$Q_a(s) = 1 + T_1 s$ $Q_b(s) = 1 + T_2 s$

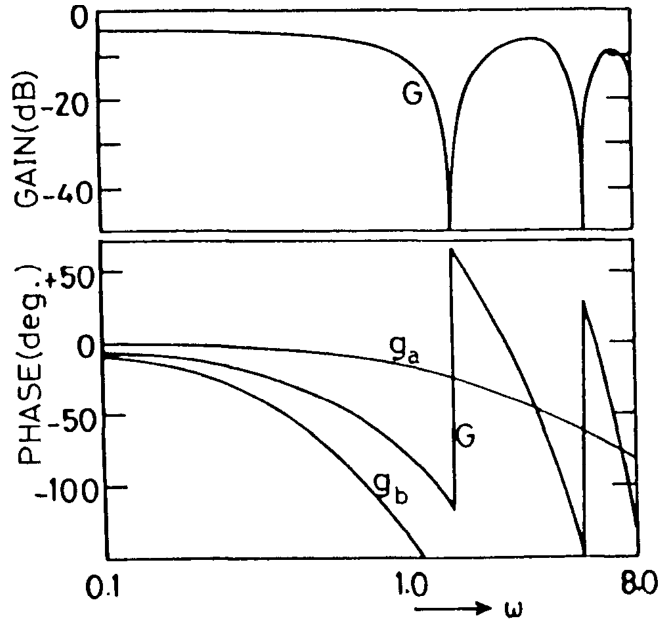

Figure 9. Frequency response of model for case [c]

$K_1 = 0.4$ $T_1 = 0.2$ $\tau_1 = 0.1$

$K_2 = 0.4$ $T_2 = 0.2$ $\tau_2 = 1.6$

$Q_a(s) = 1 + T_1 s$ $Q_b(s) = 1 + T_2 s$

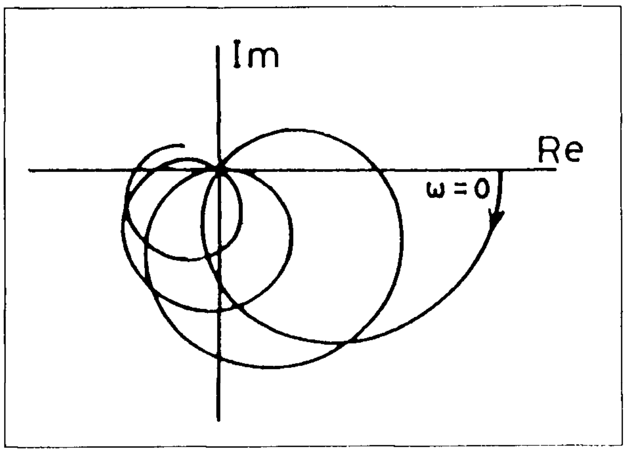

Figure 10. Vector diagram of model for case [c]

$K_1 = 0.4$ $T_1 = 0.2$ $\tau_1 = 0.1$

$K_2 = 0.4$ $T_2 = 0.2$ $\tau_2 = 1.6$

$Q_a(s) = 1 + T_1 s$ $Q_b(s) = 1 + T_2 s$

Inequality Constraints for the Appearance of Various Characteristics of Phase Angle

According to the above discussions the following inequality constraints can be written for each of the cases:
case [a]:

$$\frac{d|\angle a|/d\omega}{d|\angle b|/d\omega}<1 \text{ and } \frac{|a|}{|b|}>1\ ; \quad \omega_1 > \omega > \omega_2 \tag{14 a}$$

case [b]:

$$\frac{d|\angle a|/d\omega}{d|\angle b|/d\omega}<1 \text{ and } \frac{|a|}{|b|}<1\ ; \quad \omega_1 > \omega > \omega_2 \tag{14 b}$$

case [c]:

$$\frac{d|\angle a|/d\omega}{d|\angle b|/d\omega}<1 \text{ and } \frac{|a|}{|b|}=1\ ; \quad \omega_1 > \omega > \omega_2 \tag{14 c}$$

That is, the relative values of gains and derivatives of phase angles are the dominant parameters in the appearance of various forms of phase angle. The reason for using the derivative of phase angle is discussed below.

It is important to note that the relative value of the lengths of vectors **a** and **b** with respect to each other as well as leading and lagging of these vectors may change with an increase in ω due to the effect of parameter in $Q_a(s)$ and $Q_b(s)$. For example, if at some specific ω_g a crossing of the gains of $g_a(j\omega)$ and $g_b(j\omega)$ appears, then the form of phase angle after ω_g will change from case [a] to [b] and vice versa.

With regard to the phase angles of **a** and **b**, the change of leading and lagging of vectors **a** and **b** implies that the derivative of phase angle, which is an indication of the speed of rotation of the vector, should be applied in the inequality constraints instead of the phase angle itself. Because, if for example at the start of rotation, vector **a** is in a condition of leading with respect to **b**, then

$$|\angle a|<|\angle b| \text{ for all } \omega; \text{ if } d|\angle a|/d\omega< d|\angle b|/d\omega \text{ for all } \omega;$$

That is, if the speed of rotation of vector **a** is less than that of **b** at all frequencies then this vector **a** is in a condition of leading with respect to **b** at all frequencies.

However, if with an increase of ω, at some $\omega=\omega_p$, the speed of rotation of **a** overpasses that of **b**, then

$$d|\angle a|/d\omega< d|\angle b|/d\omega \quad \text{for } \omega<\omega_p$$

and

$$d|\angle a|/d\omega> d|\angle b|/d\omega \quad \text{for } \omega>\omega_p.$$

Therefore, after ω_p the leading and lagging condition of vectors will certainly become inverted and the form of phase angle of model will change from case [a] to case [b] or [b] to [a].

Moreover, the possibility of an appearance of some new forms of phase angle of the model is predictable. These new forms are indeed some combination of the original ones, [a] and [b]. They may be called $[ab]_g$, $[ab]_p$, $[ba]_g$, and $[ba]_p$, where the subscript "g" shows that the change in the form has occurred due to the effect of gain, and the subscript "p" is representative of the effect of phase angle. Still some more combinational forms are expected to appear. For example, if the changes of the relative values of gain and the derivative of phase angles appear both in one period then the form of phase angle will not change after that period due to the simultaneous occurrence of two changes of conditions. The forms relating to such conditions may be called $[a]_{gp}$, $[a]_{pg}$, $[b]_{gp}$ and $[b]_{pg}$. In Figures 11 and 12 two examples of frequency responses for the forms $[ab]_g$ and $[ba]_g$ are shown.

STEP RESPONSE BEHAVIOR

The step response of a general simplified model as the one in Equation 2 is

$$Y(t)= Y_a(t) + Y_b(t), \tag{15}$$

where $Y_a(t)$ and $Y_b(t)$ are responses of $g_a(s)$ and $g_b(s)$ respectively. For example, for a $G_{1,1}(s)$ model

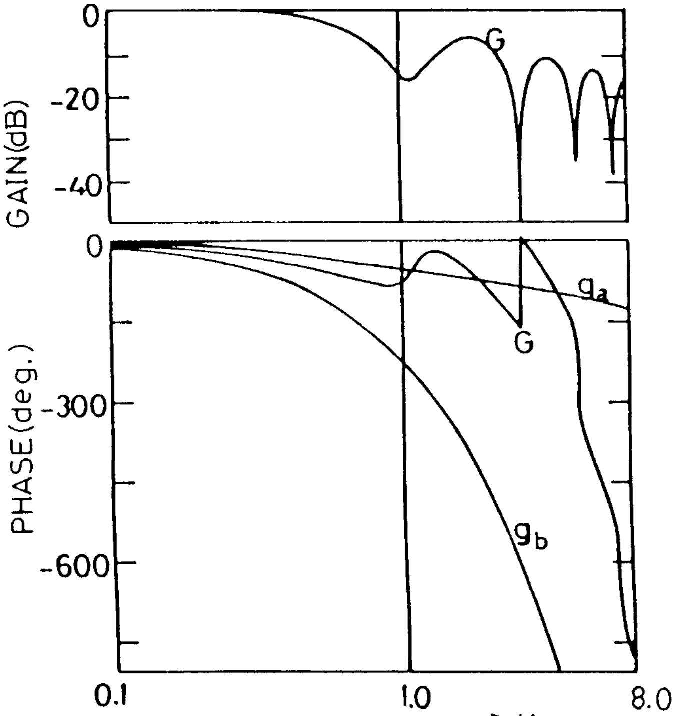

Figure 11. An example of frequency response for condition of change from case [a] to case [b] for model $G_{1,1}(s)$

$K_1 = 0.8$ $T_1 = 1.2$ $\tau_1 = 0.1$

$K_2 = 0.3$ $T_2 = 0.4$ $\tau_2 = 2.9$

$Q_a(s) = 1 + T_1 s$ $Q_b(s) = 1 + T_2 s$

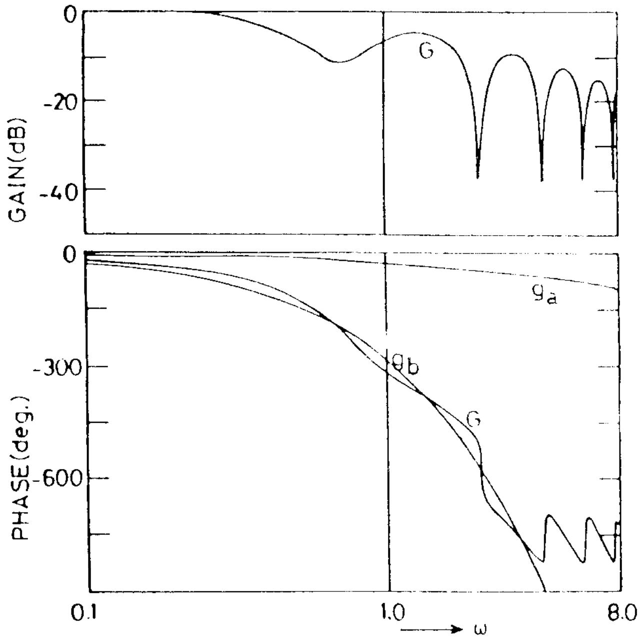

Figure 12. An example of frequency response for condition of change from case [b] to case [a] for model $G_{1,1}(s)$

$K_1 = 0.8$ $T_1 = 1.2$ $\tau_1 = 2.9$

$K_2 = 0.3$ $T_2 = 0.4$ $\tau_2 = 0.1$

$Q_a(s) = 1 + T_1 s$ $Q_b(s) = 1 + T_2 s$

$$Y_{1,1}(t) = Y_{a1}(t) + Y_{b1}(t), \qquad (16)$$

where

$$Y_{a1}(t) = K_1(1 - e^{-(t-\tau_1)/T_1}) \text{ and } Y_{b1}(t) = K_2(1 - e^{-(t-\tau_2)/T_2}).$$

The two elements $Y_{a1}(t)$ and $Y_{b1}(t)$ each will begin to effect the step response of the model just after passing a time equal to the respective time-delay in that element.

Thus if it is supposed that $\tau_1 < \tau_2$, then in total, three separate regions in step response of the model are identifiable as:

1) From t= 0 to t= τ_1 in which no response will appear from the model.

2) From $\tau = \tau_1$ up to $t = \tau_2$ in which only the step response of $g_a(s)$ is affected by input.

3) From $t = \tau_2$ up to infinite in which both $g_a(s)$ and $g_b(s)$ contribute to the response of the model. In this region an additive action of $g_a(s)$ and $g_b(s)$ appears in response.

From the above discussion it can be concluded that the actual time-delay of the model is τ_1 (the smaller time delay parameter), whereas the other one cannot be considered as the time delay of the model.

Figure 13 shows two examples for step response of a $G_{1,1}(s)$ model. In this figure the positions of parameters τ_1 and τ_2 are very well recognizable. On the contrary, in Figure 14, which is also drawn for a $G_{1,1}(s)$ model, the position of τ_2 cannot be detected explicitly.

FITTING OF THE MODEL TO SOME DISTRIBUTED PARAMETER PROCESS SYSTEMS

The simulation of a model like $G_{1,1}(s)$ to frequency response data of a counter-flow tubular one-pass heat exchanger has been reported in a previously-published paper by the authors [8]. That simulation was performed using the frequency response data that was obtained by Toudou [11] from the original complicated model of the system.

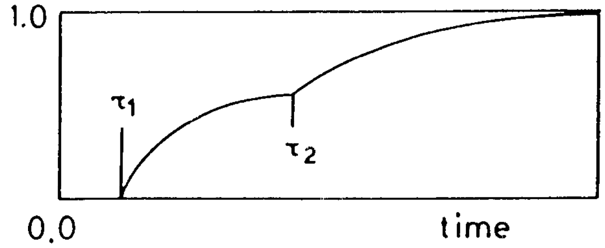

K_1= 0.6 T_1= 0.658 τ_1= 0.1
K_2= 0.4 T_2= 1.105 τ_2= 1.6

(13-a)

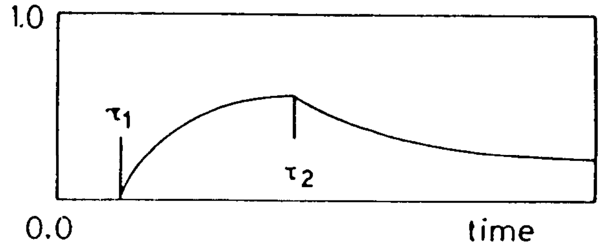

K_1= 0.6 T_1= 0.658 τ_1= 0.61
K_2= -0.4 T_2= 1.105 τ_2= 2.47

(13-b)

Figure 13. Two examples of step response of model $G_{1,1}(s)$

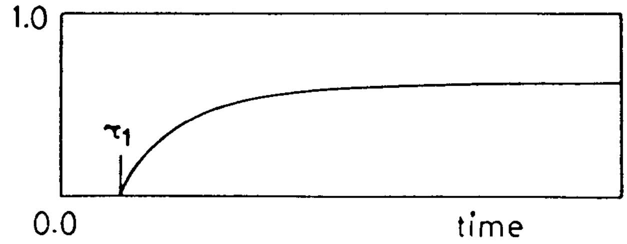

Figure 14. An example of step response of model $G_{1,1}(s)$. Position of time-delay parameters are not detectable.

K_1= 0.6 T_1= 0.658 τ_1= 0.61
K_2= 0.4 T_2= 55.0 τ_2= 2.47

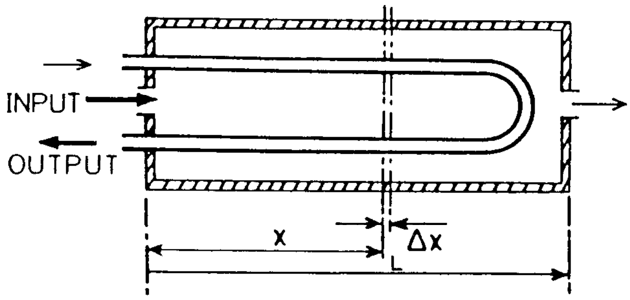

Figure 15. Two-pass shell and tube heat exchanger

In this work the results of simulations of the model to two different process systems are presented. One is performed on the complicated model of the parallel-counter flow two-pass shell and tube-heat exchanger of Matsubuchi [12,13]; the other is performed on the distributed parameter model of a fluidized bed calciner which is presented by Ramanathan [6]. Obviously, the distributed nature of heat exchangers refers to the length of the apparatus, while in the fluidized bed calciner the particle size distribution inserts the distributing nature to the process.

Fitting to Parallel-Counter Flow Two-Pass Heat Exchanger System

For the double-pass shell and tube heat exchanger the simplified model is selected to be in the form of a $G_{2,2}(s)$ transfer function.

Figure 15 shows the heat exchanger system. The frequency response data used here are from the original transfer function of the system for tube output temperature forced by shell input temperature.

The method of least squares in frequency domain was used for fitting the model to the data of the system [1,2,3]. Steepest descent method of iteration was used for calculation of the parameters of the model.

Since the data are complex numbers, if $A(\omega_i)$ is supposed to be the real and $B(\omega_i)$ the imaginary components of data at ω_i, the problem of simulation can be expressed as minimization of the summed-up amount of $e(\omega_i)^2$ in the desired range of frequency

$\omega = \omega_1$ to ω_n for i= 1,2, .., n. where

$$e(\omega_i)^2 = [A(\omega_i) - (R_a(\omega_i) + R_b(\omega_i))]^2 + [B(\omega_i) - (I_a(\omega_i) + I_b(\omega_i))]^2 \qquad (17)$$

$R_a(\omega_i)$, $R_b(\omega_i)$, $I_a(\omega_i)$ and $I_b(\omega_i)$ are real and imaginary components of $\mathbf{g_a}(j\omega_i)$ and $\mathbf{g_b}(j\omega_i)$ at ω_i.

For the general model G(s) in which $Q_a(s)$ and $Q_b(s)$

may be some irrational functions or polynomials of "s", by substitution for real and imaginary components of $\mathbf{g}_a(j\omega)$ and $\mathbf{g}_b(j\omega)$ in (17), Equation 18 will be obtained as the general form of the index of performance for simulating the simplified model of Equation 2 in frequency domain.

$$e(\omega_i)^2 = A(\omega_i)^2 + B(\omega_i)^2$$

$$+ \frac{K_1\{K_1 + 2[B(\omega_i)\,U_a(\omega_i) + A(\omega_i)\,V_a(\omega_i)]\sin(\omega_i\tau_1)\}}{U_a^2(\omega_i) + V_a^2(\omega_i)}$$

$$- \frac{2K_1[A(\omega_i)\,U_a(\omega_i) - B(\omega_i)\,V_a(\omega_i)]\cos(\omega_i\tau_1)}{U_a^2(\omega_i) + V_a^2(\omega_i)}$$

$$+ \frac{K_2\{K_2 + 2[B(\omega_i)\,U_b(\omega_i) + A(\omega_i)\,V_b(\omega_i)]\sin(\omega_i\tau_2)\}}{U_b^2(\omega_i) + V_b^2(\omega_i)}$$

$$- \frac{2K_2[A(\omega_i)\,U_b(\omega_i) - B(\omega_i)\,V_b(\omega_i)]\cos(\omega_i\tau_2)}{U_b^2(\omega_i) + V_b^2(\omega_i)}$$

$$+ \frac{2K_1K_2[U_a(\omega_i)\,U_b(\omega_i) + V_a(\omega_i)\,V_b(\omega_i)]\cos[\omega_i(\tau_1 - \tau_2)]}{[U_a^2(\omega_i) + V_a^2(\omega_i)]\,[U_b^2(\omega_i) + V_b^2(\omega_i)]}$$

$$- \frac{2K_1K_2[U_b(\omega_i)V_a(\omega_i) - U_a(\omega_i)V_b(\omega_i)]\sin[\omega_i(\tau_1 - \tau_2)]}{[U_a^2(\omega_i) + V_a^2(\omega_i)]\,[U_b^2(\omega_i) + V_b^2(\omega_i)]} \quad (18)$$

Here, $U_a(.)$, $U_b(.)$, $V_a(.)$ and $V_b(.)$ are real and imaginary components of $\mathbf{Q}_a(j\omega_i)$ and $\mathbf{Q}_b(j\omega_i)$ respectively. For this problem since the model is a "2,2" order model then

$$U_a(\omega_i) = 1 - T_1^2\omega_i^2 \;,\quad V_a(\omega_i) = 2\zeta_1 T_1\omega_i$$

$$U_b(\omega_i) = 1 - T_2^2\omega_i^2 \;,\quad V_b(\omega_i) = 2\zeta_2 T_2\omega_i.$$

Figure 16 represents the basic concept which is used for obtaining the index of performance in frequency domain. That is, minimization of the lenght of vector $\Delta G(j\omega)$ which is the difference vector between the vectors of the original model and the simplified model. Figure 17 shows the results of simulation.

In this example, simulation was performed on the range of ω from 0.1 to 5.7 and in this range n= 57 points were used (ω_i= 0.1, 0.2, 0.3, ... , 9.9, 5.7). The amount of calculated parameters are

$K_1 = 0.3172$ $T_1 = 0.5062$ $\zeta_1 = 0.6706$ $\tau_1 = -0.3090$
$K_2 = 0.2137$ $T_2 = 0.2496$ $\zeta_2 = 1.6912$ $\tau_2 = 1.6278$

The summation of the errors between the simplified model and the original data (calculated from Equation 2 for 57 points) is E_{pc} = 0.032407.

Fitting of the Model to Fluidized-Bed Calciner System

The fluidized-bed calciner system which is used here for simulation is the Dorr-Oliver fluo-solids lime-mud reburning calciner [14].

Control of the particle-size distribution can be achieved through measuring the cumulative mass fraction above a cut point size. The dynamics of particle size distribution in this system can be modeled using a population balance on particles. The transfer function for the cumulative mass fraction above a cut point size "Z" is presented by Ramanathan [6] as:

$$G_p(s) = \frac{[P_z(s)/P_z(0)]\,e^{-zs} - 1}{s(s+1)(s^2+3s+3)}, \quad (19)$$

where

$P_z(s) = (s+1)^3Z^3 + 3(s+1)^2Z^2 + 6(s+1)Z + 6$
$P_z(0) = Z^3 + 3Z^2 + 6Z + 6.$

The cut point size 'Z" is cumulative mass fraction cut point size which is selected to be equal to 2 in this example. The time and cumulative mass fraction "Z" are the parameters of this distributed parameters system.

The form of equation is not as complicated as liquid-

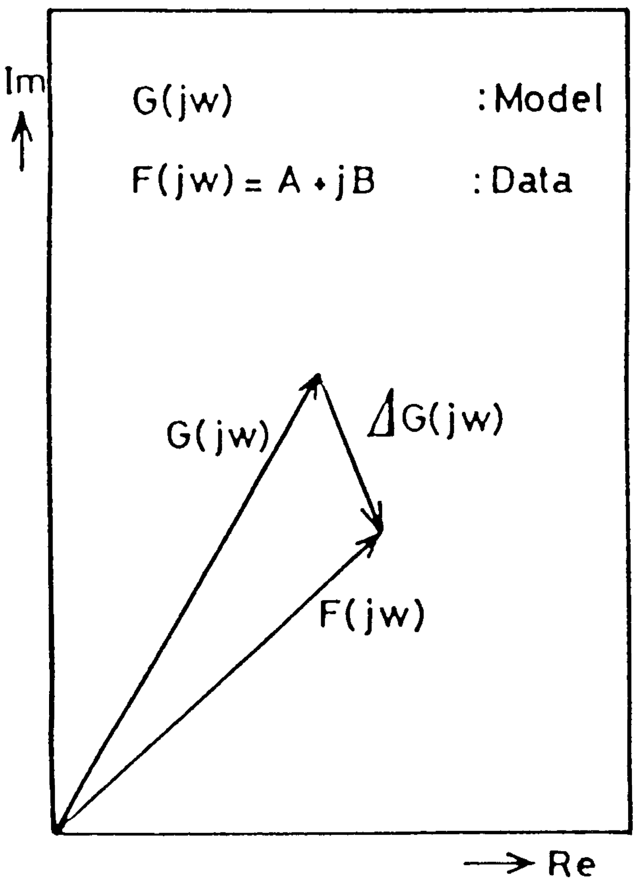

Figure 16. Minimization of the length of difference vector between the vector of model and data can be used for simulating the model to frequency response data of system.

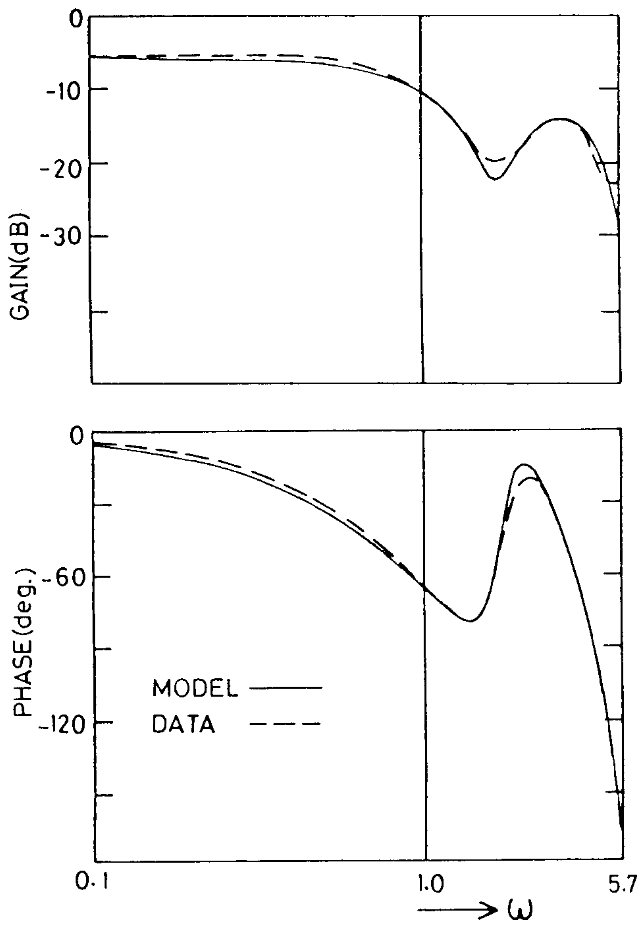

Figure 17. Result of simulation of $G_{2,2}(s)$ simplified model to frequency response data of parallel-counter flow shell and tube heat exchanger

simplification is done by fitting a $G_{2,1}(s)$ model on the step response data of the original model. The results of simulation are presented in Figure 18.

This system has negative gain with the final value tending to -0.1403. The number of parameters to be calculated were reduced from seven to six by use of the concept of $K_1 + K_2 =$ const. which is determined straightly from the steady state region of step response data. The results of calculations are

$K_1 = -10.012$ $T_1 = 5.918$ $\zeta_1 = 4.743$ $\tau_1 = 0.620$

$K_2 = 9.871$ $T_2 = 55.900$ ______ $\tau_2 = 2.000$

The summation of errors for 33 points of time $\tau_i = 0.0, 0.25, 0.50, \ldots, 8.0$ was $E_f = 0.00007477$. The frequency response of both the simulated model and original one are shown in comparison with each other in Figure 19.

CONCLUSIONS AND DISCUSSIONS

Frequency response investigation of the proposed general simplified model of Equation 2 confirms the capability of the model for describing the transcendental dynamical characteristics of a class of distributed parameter process systems that can be described by hyperbolic form of partial differential equations. In these systems, that frequently appear in chemical process industries, the convective transport dominates the dispersive phenomena [6]. The important yet complicated specific characteristics of these systems (especially in frequency domain) are detected from the general formulations of frequency response and complex plane representation of the model.

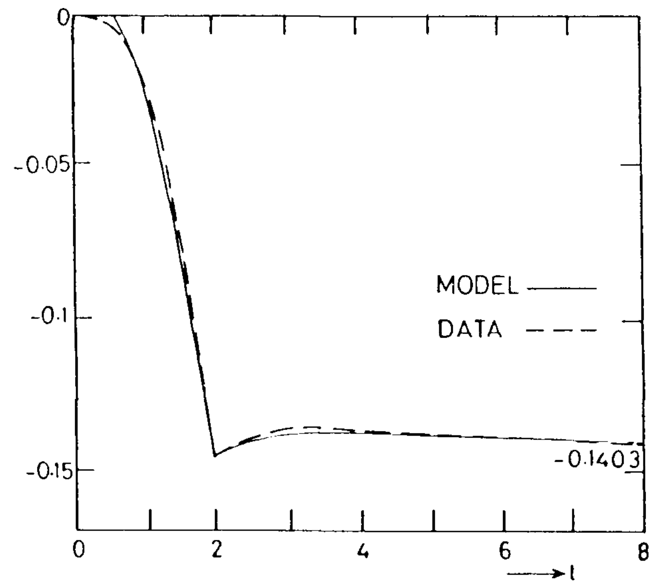

Figure 18. Result of the time domain simulation of the model to the fluidized bed calciner

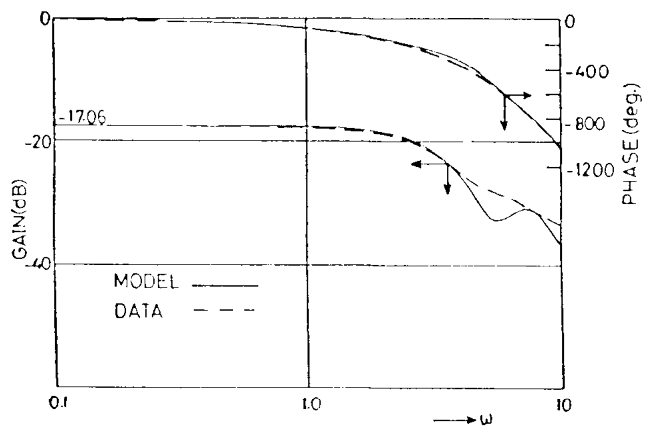

Figure 19. Frequency response of the simulated simplified model and the original model of the fluidized bed calciner

Concerning the characteristics of gain for a model $G_{m,n}(s)$:

1) At any frequency "ω" the width of the resonances of gain (that is, the distance between the upper and lower envelopes of gain) is equal to two times the gain of "smaller gain element" in the model. That is, the gain of "smaller gain element" at each "ω" fixes the difference between upper and lower envelopes.

2) If the order of elements of model $g_{am}(s)$ and $g_{bn}(s)$are equal; say m=n=u, then on the log-log scale of gain the two asymptotes are parallel lines with slopes equal to -20u dB/dec.

3) The parameter $\tau_1 - \tau_2 = \tau$ is the main effective variable which specifies the regular periods of gain at sufficiently high frequencies. Whilst at sufficiently high frequencies the effects of phase angles of the terms $1/Q_a(j\omega)$ and $1/Q_b(j\omega)$ are almost diminished.

Concerning the phase angle of the model:

1) The period of oscillation of phase angle is equal to the period of gain.

2) Three basic forms (or cases [a], [b] and [c]), are revealed from complex plane representation of the model, and many other forms can possibly appear from the combination of these three forms. Such forms will appear due to the crossing of the gains and/or change of speed of rotation of vectors of the individual elements of model $g_a(s)$ and $g_b(s)$, with respect to each other.

In the example of two-pass shell and tube heat exchanger the phase angle of the system is similar to the form $[ab]_g$ while the example of fluidized bed calciner shows a phase angle of the form [b] which is a nonminimum phase system. On the other hand, the results of simulation of a model $G_{1,1}(s)$ to the counter-flow tubular heat exhanger which was previously published by the authors [8], represents the form of phase angle in case [a]. At the same time, it is notable that the model of a Mixed Suspension Mixed Product Removal Crystallizer for the cumulative mass transfer function with respect to inlet concentration which is introduced by Ramanathan [4] is an actual example for the form $[ba]_g$ of phase angle.

In the above examples the order of the model was selected by trial and error so that the best fitness could be obtained with a relatively low order model. However, the results of the simulations were excellent both in the frequency domain and in the time domain.

In all three examples regardless of the employed type of data (frequency domain or time domain) the number of parameters that must be calculated can be reduced by one, since $K_1 + K_2 = K =$ constant, can be predicted straightly from the data. This means that a complete fitness of the model at steady-state and/or in very low frequencies is exerted in the simulation procedures.

Moreover, the results of this work may be used in controlling the distributed parameter systems. In this respect, the conclusions regarding the characteristics of phase angle seem to be of importance and are helpful as a guideline for further studies.

REFERENCES

1. E.C. Levy: Complex-Curve Fitting, *IRE* Trans. on Automatic Control, AC-4, 37, May (1959).
2. C.K. Santanon and J. Koerner: Transfer Function Systems as a Ratio of Two Polynomials, *IEEE* Trans. Automatic Control, AC-8, 56 (1963).
3. D.E. Seborg, T.F. Edgar and D.A. Mellichamp: "Process Dynamics and Control," John Wiley (1989).
4. S. Ramanathan, R.L. Curl and C. Kravaris: " Dynamics and Control of Quasirational Systems," *AIChE J.*, 35-6, 1017 (1989).
5. S. Ramanathan, R.L. Curl and C. Kravaris: " Dynamics and Control of the Cumulative Mass Fraction of a Particle Size Distribution," ACC Proc., Minneapolis, June, (1987).
6. S. Ramanathan: Control of Quasirational Distributed Systems with Examples on the Control of Cumulative Mass Fraction of a Particle Size Distribution, PhD Thesis, Unv. of Michigan (1988).
7. M. Kuramac and T. Kobayashi: Preprint Soc. Chem. Engs. Japan, Kantoushibu, Niigata, B105, 67 (1988) (in Japanese).
8. M. Shirvani, M. Inagaki and T. Shimizu: On a Transfer Function that Approximates Complex Dynamics, *Kagaku Kogaku Ronbunshu*, 18-6, 862 (1992) (in Japanese).
9. M.J. Bosley and F.P. Lees: A Survery of Simple Transfer-Function Derivations from High-Order State Variable Models, *Automatica*, 8, 765 (1972).
10. A. Hempel: On the Dynamics of Steam Liquid Heat Exchangers, Trans. *ASME*, Ser. D, 83-2, 244 (1961).
11. I. Toudou: "Flow Forced Dynamic Behavior of Heat Exchangers," Trans. *JSME*, 33, 1215 (1967) (in Japanese).
12. M. Masubuchi: Control of Multipass Heat Exchangers (part I) -Dynamic Characteristics of Two Pass Heat Exchangers, Trans. *JSME* 24, 139; 209 (1958) (in Japanese).
13. M. Matsubuchi: Dynamic Response and Control of Multipass Heat Exchangers, Trans. *ASME*, Basic Eng., 51, March (1960).
14. J. Moran and C. Wall: Int. Alkaline Pulping Conf., Murray Bay, P. Q., Canada (1965).